Calorie restriction induces mitochondrial biogenesis and bioenergetic efficiency

G. López-Lluch*, N. Hunt†, B. Jones†, M. Zhu†, H. Jamieson‡§, S. Hilmer‡§, M. V. Cascajo*, J. Allard†, D. K. Ingram†, P. Navas*, and R. de Cabo†¶

*Centro Andaluz de Biología del Desarrollo, Universidad Pablo de Olavide, 41013 Sevilla, Spain; †Laboratory of Experimental Gerontology, National Institute on Aging, National Institutes of Health, 5600 Nathan Shock Drive, Baltimore, MD 21224-6825; ‡Centre for Education and Research on Aging, University of Sydney, Concord Hospital, Concord NSW 2139, Australia; and §Departments of Aged Care and Clinical Pharmacology, Royal North Shore Hospital, St. Leonards NSW 2069, Australia

Communicated by J. Edwin Seegmiller, University of California at San Diego, La Jolla, CA, December 8, 2005 (received for review October 20, 2005)

Age-related accumulation of cellular damage and death has been linked to oxidative stress. Calorie restriction (CR) is the most robust, nongenetic intervention that increases lifespan and reduces the rate of aging in a variety of species. Mechanisms responsible for the antiaging effects of CR remain uncertain, but reduction of oxidative stress within mitochondria remains a major focus of research. CR is hypothesized to decrease mitochondrial electron flow and proton leaks to attenuate damage caused by reactive oxygen species. We have focused our research on a related, but different, antiaging mechanism of CR. Specifically, using both *in vivo* and *in vitro* analyses, we report that CR reduces oxidative stress at the same time that it stimulates the proliferation of mitochondria through a peroxisome proliferation-activated receptor coactivator 1α signaling pathway. Moreover, mitochondria under CR conditions show less oxygen consumption, reduce membrane potential, and generate less reactive oxygen species than controls, but remarkably they are able to maintain their critical ATP production. In effect, CR can induce a peroxisome proliferation-activated receptor coactivator 1α-dependent increase in mitochondria capable of efficient and balanced bioenergetics to reduce oxidative stress and attenuate age-dependent endogenous oxidative damage.

aging | peroxisome proliferation-activated receptor coactivator 1 | reactive oxygen species

One of the major hypotheses directing gerontological research over several decades is that aging results from the accumulation of macromolecules damaged by oxidative stress and that the major loci of this damage is the mitochondrion (1–4). This hypothesis has been proposed as one explanation of how calorie restriction (CR) in various animal models works so effectively to increase lifespan and stress resistance, reduce susceptibility to chronic disease, and attenuate age-related functional decline (5, 6). Past studies have demonstrated that CR decreases mitochondrial electron and proton leak in mammalian cells and attenuates damage resulting from intracellular oxidative stress (4, 6–9).

Mitochondria provide an integrated functional network, many components of which are vulnerable to oxidative stress that can impair cellular function and increase the chance of cell death. Age-related accumulation of cellular damage and death ultimately leads to impaired organ function generating further physiological dysfunction (1, 2). The mitochondrial theory of aging proposes that somatic mutations of mtDNA induced by reactive oxygen species (ROS) are the primary cause of cellular energy decline with complex I being particularly affected by decreasing its rate of electron transport (3).

CR is the most robust, nongenetic intervention that increases lifespan and reduces the rate of aging in mammals and other organisms (5, 7). The mechanisms responsible for the antiaging effects of CR remain unknown and likely involve several processes. Results from many different laboratories support that both the activation of cell survival mechanisms and decreased mitochondria-dependent ROS production are major factors accounting for the antiaging effects of CR (6, 7). In fact, lifespan is inversely related to the rate of mitochondrial hydroperoxide production (4) that has been reported to increase with aging and decrease with CR (6, 8). Experiments in which transgenic animals were produced that overexpress specific antioxidant enzymes, particularly catalase expressed in mouse mitochondria (10) and catalase and copper, zinc superoxide dismutase (SOD) in fruit fly (11, 12), have demonstrated significant lifespan extension. Respiration has also been considered to play a key role in the antiaging effects of CR (13). Evidence for this mechanism has been confirmed by observations of significant CR-dependent increase of expression of genes involved in mitochondrial energy metabolism (14). However, recently conflicting results about the effect of CR on mitochondrial physiology have been shown (15–17).

We propose that CR improves energy production through a balanced respiration maintaining lower oxygen consumption associated with low ROS production. To evaluate this hypothesis, we have used the *in vitro* model of CR, which has proven useful for demonstrating mechanisms of cell survival induced by this intervention (18, 19). Using this approach, we have used various assays to determine whether mitochondrial mass and function are increased in human and rat cells treated with serum from CR rats. We have also examined tissues from CR rats to further confirm these observations. Our results provide definitive evidence of a major cellular change in which CR induces a greater number of more efficient mitochondria.

Results and Discussion

To investigate whether the CR-dependent decrease of mitochondrial ROS production is reproduced *in vitro*, HeLa cells, FaO cells, and primary hepatocytes were incubated in the presence of serum from rats submitted to long-term CR (40% for 6–12 months) and compared with those incubated with serum from age-matched, ad libitum (AL)-fed rats (18). Results from this *in vitro* model of CR showed a clear decrease of intracellular fluorescence signals for ROS forms as determined by carboxy-2′,7′-dichlorodihydrofluorescein diacetate (cH_2DCFDA) and dihydroethidium (Het) (Fig. 1*A*). Thus, a significant decrease in ROS production in CR cells was observed when compared with cells grown in AL serum (Fig. 1*B*). The decrease of ROS production could not be attributed to changes in antioxidant enzyme expression as demonstrated by the levels of

Conflict of interest statement: No conflicts declared.

Freely available online through the PNAS open access option.

Abbreviations: AL, ad libitum; cH_2DCFDA, carboxy-2′,7′-dichlorodihydrofluorescein diacetate; CR, calorie restriction; $\Delta\Psi$m, mitochondrial membrane potential; HET, dihydroethidium; JC1, 5,5′,6,6′-tetrachloro-1,1′,3,3′-tetraethylbenzimidalolylcarbocyanine iodide; MFI, mean fluorescence intensity; MTG, mitotracker green FM; NaO, nonyl acridine orange; NRF, nuclear respiratory factor; PPAR, peroxisome proliferation-activated receptor; PGC-1, PPAR coactivator 1; ROS, reactive oxygen species; SIRT, Sir2 homolog; SOD, superoxide dismutase.

¶To whom correspondence should be addressed. E-mail: decabora@grc.nia.nih.gov.

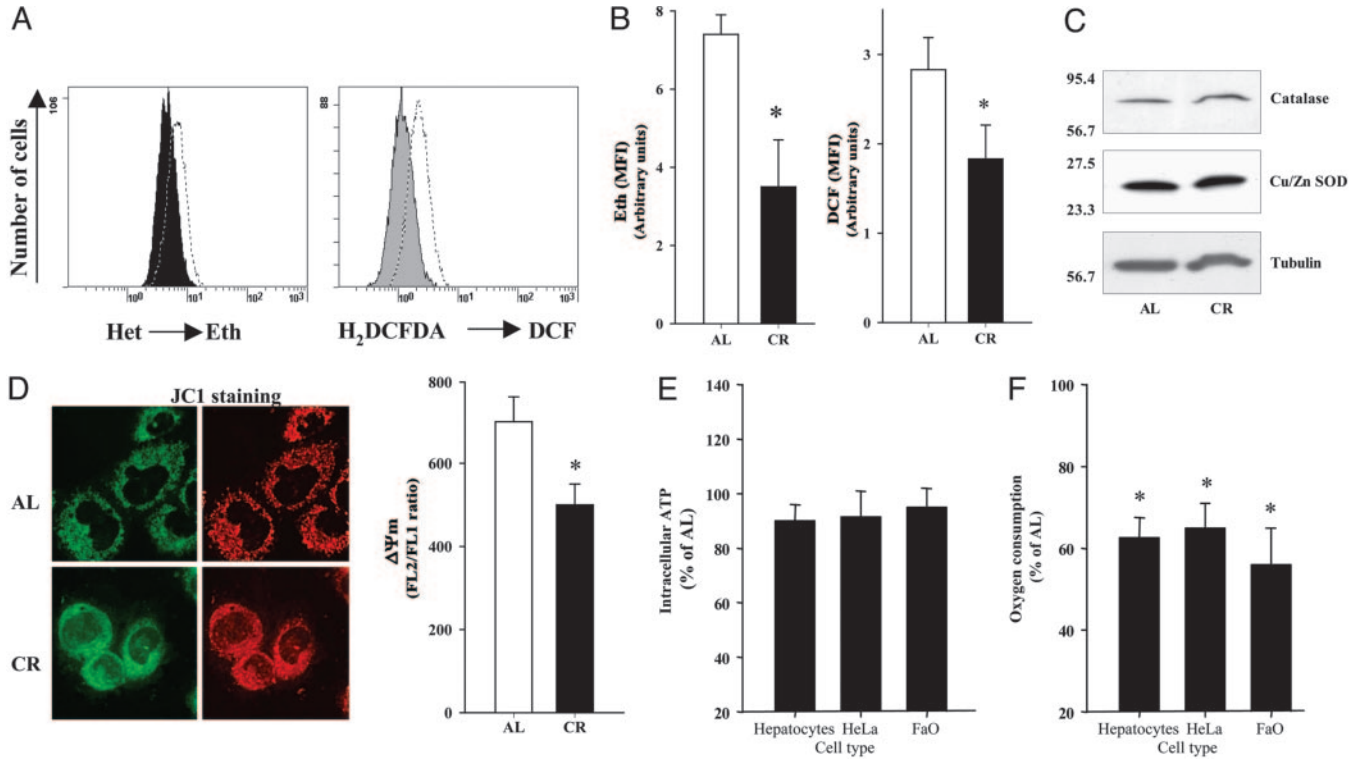

Fig. 1. ROS in HeLa cells cultured under AL and CR serum conditions. Oxidation of Het or cH_2DCFDA in cells cultured after 48 h with AL or CR sera was determined separately by flow cytometry as indicated in *Methods*. (*A*) Histogram distribution from a significant experiment of each determination. Dotted histogram corresponds to AL cells, and filled histogram corresponds to CR cells. Eth, ethidium; DCF, dichlorofluorescein. (*B*) Data indicate the mean of the mean fluorescence intensity (MFI) from three different experiments performed in duplicate. *, Significant differences vs. AL treatment, $P < 0.01$. (*C*) Protein levels of catalase and Cu/Zn SOD. Western blots were performed as described in *Methods*. (*D*) ΔΨm in HeLa cells cultured under AL and CR conditions after 48 h was determined by using JC1 as indicated in *Methods*. (*Left*) Confocal images of JC1-stained cells after treatment. Images were acquired by using a ×63 objective. (*Right*) Ratiometric analysis of the fluorescence of JC1-aggregated form (FL2) vs. JC1-free form (FL1) from three different experiments performed in duplicate. *, Significant differences vs. AL treatment, $P < 0.01$. (*E* and *F*) Intracellular ATP levels (*E*) and oxygen consumption (*F*) in cells after 48 h of incubation. *, Significant differences vs. AL oxygen consumption, $P < 0.01$.

both catalase or Cu/Zn SOD in whole cell extracts (Fig. 1*C*). These data obtained by our *in vitro* system confirm the previous results showing decreased ROS production in mitochondria induced by *in vivo* CR experiments (6, 8, 20). Our results contradict the recent results of Lambert and Merry (16) showing that CR did not affect bioenergetics or ROS production in intact rat hepatocytes isolated from CR rats. This discrepancy may be caused by differences in the dietary regimen and methods used for ROS determination in both studies but also because we have treated cells *in vitro* with CR serum, whereas the hepatocytes in the Lambert and Merry study were isolated from CR rats and grown in Hanks' balanced salt solution (HBSS).

Because the mitochondrial membrane potential (ΔΨm) is the central bioenergetic parameter controlling the generation of ROS (1), we examined the ΔΨm signal by using 5,5′,6,6′-tetrachloro-1,1′,3,3′-tetraethylbenzimidalolylcarbocyanine iodide (JC1) in HeLa cells treated with either CR or AL sera (Fig. 1*D*). After 48 h, ratiometric analysis of JC1-aggregated forms vs. the free form demonstrates that a lower ΔΨm in these cells was confirmed by direct visualization by confocal microscopy. Then, incubation with CR serum seems to decrease ΔΨm in these cells. Our *in vitro* results confirmed previous *in vivo* data showing a CR-dependent decrease of ΔΨm in liver mitochondria caused by decreased mitochondrial respiration together with increased proton leak (20). It has been demonstrated that the probability of electron leakage to form superoxide increases at high ΔΨm (1, 21, 22). Our results show that CR slowed down both ΔΨm and ROS. Do these findings necessarily mean a lower rate of O_2 consumption or a lower ATP production in CR cells? Based on previous studies of basal metabolism of rodents measured as oxygen consumption, it is expected that short-term CR will reduce metabolic rate, but that in long-term measurements, the metabolic rate of CR animals will not differ significantly from that of AL controls because of changes in body composition (23, 24). In the current *in vitro* analysis of CR serum-treated cells and isolated hepatocytes, the levels of ATP (Fig. 1*E*) or the ATP/ADP ratio (Fig. 4, which is published as supporting information on the PNAS web site) were not significantly different compared with AL controls. Interestingly, we observed that oxygen consumption compared with AL conditions was reduced by 35–40% in a variety of cells grown in CR serum and in freshly isolated primary hepatocytes from 1-yr-old CR rats (Fig. 1*F*). Part of this decrease in oxygen consumption could be caused by the minor ROS production by mitochondria together with a lower respiration rate (15).

Thus, our results support the proposal that CR produces very efficient electron transport through the respiratory chain, that is, equivalent ATP production under conditions of lower oxygen consumption and ROS production. This change in mitochondrial efficiency could attenuate molecular and cellular damage resulting from oxidative stress and thus reduce the rate of aging at cellular and organismic levels (25, 26). Our results agree with previous findings in isolated mitochondria from liver from rats fed under CR conditions that show lower respiration and higher proton leak at the same time (15). This fact would explain the lower oxygen consumption and the decrease of ΔΨm at the same time. However, recent studies have reported the reduction of mitochondrial ROS produc-

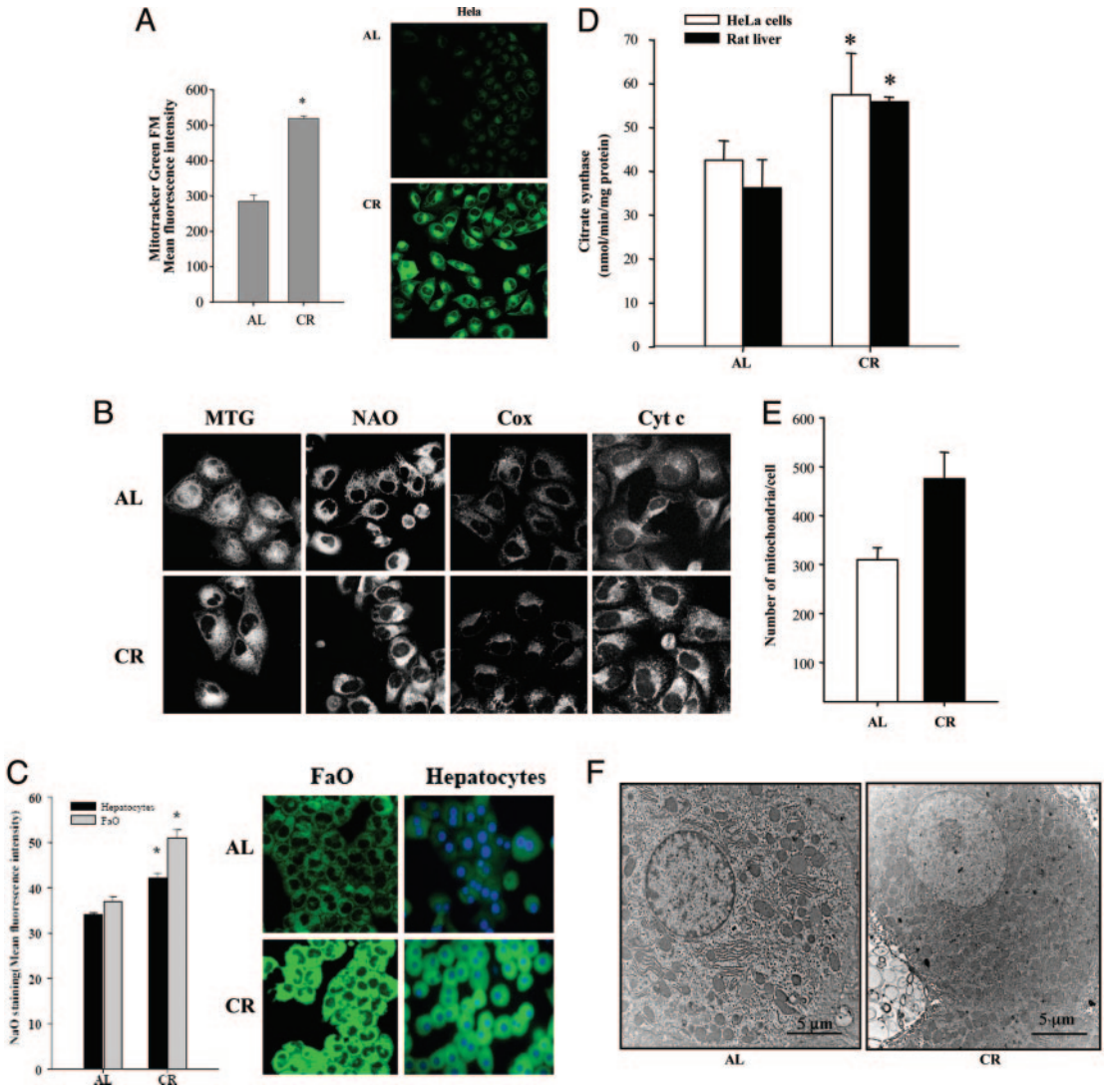

Fig. 2. Mitochondrial mass and distribution in HeLa cells cultured under AL and CR serum conditions. (*A*) Mitochondrial mass in cells cultured after 48 h with AL or CR sera was determined by flow cytometry by using MTG as indicated in *Methods*. (*Left*) Data indicate the mean of the MFI from three different experiments performed in duplicate. *, Significant differences vs. AL treatment, $P < 0.01$. (*Right*) MTG signal in AL and CR cells visualized by confocal microscopy. Images were acquired by using a ×40 objective. Settings for detectors were maintained along the study. (*B*) Mitochondrial staining in HeLa cells cultured under AL and CR serum conditions. Representative images of mitochondrial staining in AL and CR cells by using 20 nM MTG, 10 μM NAO, and immunostaining with anticytochrome *c* (Cyt c) or anticytochrome *c* oxidase I (Cox). Images were acquired by using a ×63 objective. (*C*) NAO staining of FAO and primary rat hepatocytes cultured in AL and CR conditions. (*Left*) Data indicate the mean of the MFI from three different experiments performed in duplicate. *, Significant differences vs. AL treatment, $P < 0.01$. (*Right*) NAO signal in AL and CR cells visualized by confocal microscopy. Images were acquired by using the ×40 objective. (*D*) Citrate synthase activity in HeLa cells incubated with rat serum grown under AL or CR conditions and from rat liver from animals fed under these conditions for 8 months. *, Significant differences vs. AL treatment, $P < 0.01$. (*E*) Quantification of the mitochondrial numbers from micrographs of 24-month-old AL and CR rat hepatocytes as described in *Methods*. *, Significant differences vs. AL treatment, $P < 0.01$. (*F*) EM of AL (*Left*) and CR (*Right*) rat hepatocytes prepared and imaged as described in *Methods*.

tion by the decrease of proton leak and a higher $\Delta\Psi$m in CR mitochondria (16). Both studies are based on *in vitro* analysis of isolated mitochondria. Our cytometrical approach permits us to determine $\Delta\Psi$m and ROS in the living cell environment without isolation procedures and buffer disturbances that could have impacted the conclusions drawn from past studies.

The next question to ask then is how does the cell increase this respiratory efficiency? We hypothesize that CR supports efficient respiration by increasing the number of low potential mitochondria (state 3). To investigate this hypothesis, we incubated HeLa cells, FaO cells, and rat primary hepatocytes in sera obtained from rats on either CR or AL diets and analyzed the cells for different mitochondrial markers after this exposure. HeLa cells incubated with CR serum showed a significant increase of mitotracker green FM (MTG) signal, indicating the increase of mitochondrial mass (Fig. 2*A*). This fact was confirmed by using the nonyl acridine orange (NaO) probe, which specifically binds to cardiolipin, a mitochondrial-specific phospholipid and is widely considered a mitochondrial mass marker (Fig. 2*B*). Immunolocalization of both cytochrome *c* and cytochrome *c* oxidase in CR sera-treated HeLa cells also confirmed the increase of mitochondria compared with AL-treated cells (Fig. 2*B*) and the specificity of MTG and NaO staining as determined by the mitochondrial staining pattern (Fig. 2*B*). Both FaO cells incubated with CR serum and primary hepatocytes isolated from rats fed under CR long term also showed a significant increase of cardiolipin-dependent NaO staining signal

(Fig. 2*C*), indicating that this CR effect seems to be independent of cell type.

Citrate synthase activity is also considered a biomarker of mitochondrial mass and function. Reduced activity of this enzyme has been observed in livers from aged AL rats and is attenuated by CR (27). Activity of citrate synthase was increased significantly in CR sera-treated cells compared with AL conditions and in CR liver compared with AL tissue (Fig. 2*D*).

To confirm an actual increase in the number of mitochondria, we next conducted an EM analysis of mitochondria in liver tissue obtained from old AL and CR rats. We could detect a significant increase in the number of mitochondria in this tissue (Fig. 2*E*), which was quantified from EM micrographs as represented in Fig. 2*F*. Thus, based on a variety of assays to determine mitochondrial mass in different cell types, the results would support the hypothesis that CR increases the number of mitochondria per cell.

Taken together, these results support the conclusion that a larger amount of low-potential mitochondria would maintain a balanced respiratory chain activity fully capable of handling reduced oxygen consumption while maintaining ATP synthesis but with a lower ROS production. In fact, the mitochondrial protein density in liver, which can be interpreted as a marker of mitochondrial mass, is increased in CR rats without any change in the respiration rate (17). All of these results are in agreement with the fact that CR reduces body temperature in mammals (28), which may be caused by increased coupling of oxidative phosphorylation to ATP synthesis (29). The increase of CR-dependent low-potential mitochondria would explain these previously well established observations.

Having established that CR can up-regulate mitochondria and improve metabolic efficiency, questions emerge regarding what processes are involved in this up-regulation. Mitochondrial biogenesis is a highly regulated process operating through peroxisome proliferation-activated receptor (PPAR) coactivator 1 α (PGC-1α)-dependent nuclear respiratory factors (NRFs). Interestingly, recent reports suggest a role for Sir2 homolog (SIRT) in the regulation of PGC-1α during CR and fasting (13, 30, 31). We have previously shown an induction of SIRT1 in cells and tissues under CR and stress conditions (18, 19). To investigate how CR can induce a greater number of low-potential mitochondria, we determined the expression of mRNA of NRF1 and NRF2, which control the expression of nuclear genes that codify most of the subunits of mitochondrial complexes (32–34), and PPARα, another factor that would contribute to mitochondrial biogenesis by the activation of the fatty acid oxidation pathway (35). The expression of the respective mRNAs was determined by RT-PCR in HeLa cells incubated for 24 h with both AL and CR serum. Both NRF1 and NRF2$\beta\gamma$ transcripts were significantly increased in CR serum-treated cells compared with AL serum-treated cells; whereas, NRF2α did not show any significant change of expression (Fig. 3*A*). PPARα was not induced by CR serum treatment *in vitro* (Fig. 3*A*), and these results agree with previous ones showing that this factor is not activated in rat kidney and liver by short-term CR treatment *in vivo* (36, 37). On the other hand, both induced factors, NRF1 and NRF2, are involved in mitochondrial biogenesis under conditions that promote increased respiration (34, 38). In both cases, NRF1 and NRF2 depend on PGC-1α transcriptional coactivator (33), which is up-regulated by both short- and long-term CR (36). In our hands, *in vivo* expression of PGC-1α and PPARα were elevated in livers from 1-year-old CR rats compared with AL-fed rats (Fig. 3*B*). In agreement with this finding we have shown previously an activation of PGC-1α and some of its downstream targets in liver of CR rats ranging from 12 to 24 months of age (36).

Several of the effects of CR serum on cultured cells have been linked to low levels of insulin. In fact, the resistance of cells to heat shock and the induction of SIRT1 expression in cells cultured in the presence of serum from rats fed under CR conditions were inhibited by the addition of insulin to the culture medium (18, 19). In our hands, the addition of insulin to CR-serum cultures also inhibited

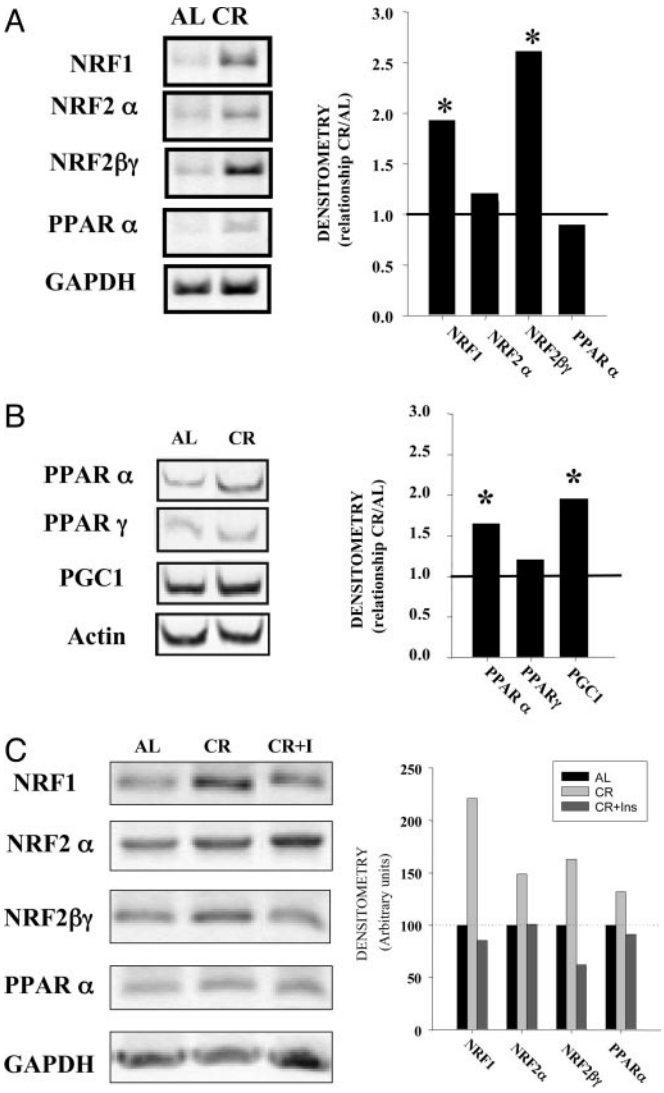

Fig. 3. Regulation of mitochondrial biogenesis. (*A*) Expression of mitochondrial biogenesis factors determined by RT-PCR in HeLa cells. Total RNA from cells cultured during 48 h with 10% AL or CR sera was extracted, and the amount of specific mitochondrial factors was determined by RT-PCR as indicated in *Methods*. The average intensity of each product was related to the control gene GAPDH or β-actin. These ratios were then used to calculate relative mRNA levels by densitometry. (*Left*) A representative image of blots from three different experiments is shown. (*Right*) Data represent the mean of the relationship between the mRNA from CR samples and AL samples from at least three different experiments. *, Significant increase of blots in CR samples vs. AL samples, $P < 0.05$. (*B*) Expression of mitochondrial biogenesis factors in rat liver. Samples from AL- and CR-fed rats were processed as indicated in *Methods*, and the expression of mitochondrial biogenesis factor mRNA was determined as above. *, Significant increase in CR samples, $P < 0.05$. (*C*) Effect of insulin on mitochondrial biogenesis markers induced by CR on HeLa cells. Samples were processed as in *A*.

the induction of NRF1 and NRF2$\beta\gamma$ mRNA (Fig. 3*C*), suggesting that the insulin-dependent pathway is involved in the regulation of the mitochondrial changes induced by CR serum.

In numerous experiments, the SIRT1 pathway has been shown to be involved in the antiaging mechanisms of CR, particularly in the protection against stress (13, 19). The CR mechanism identified in the current investigation differs from that induced *in vitro* in response to fasting and pyruvate wherein SIRT1 deacetylates PGC-1α and induces the expression of gluconeogenic genes but not mitochondrial genes (31).

The antiaging effect of CR in mammals is a multidimensional phenomenon that must be highly regulated (39). The *in vitro* model of CR has helped to clarify the SIRT1-dependent regulatory pathway that enhances stress resistance in a wide variety of organisms (18, 19). Another basic aspect of the antiaging effects of CR is a decrease of endogenous oxidative stress production mainly in mitochondria, which would prevent the accumulation of damage (6, 8, 40). Our current study demonstrates that this effect can be caused by a PGC-1α-dependent mechanism that increases mitochondrial mass. These mitochondria show a low-membrane potential, under lower oxygen consumption without diminishing ATP production, and generate lower levels of ROS, thus attenuating damage caused by endogenous oxidative stress and maintaining a balanced respiratory chain. PGC-1α or SIRT1 are critical to regulate this response. As evidence for their role, we disrupted expression of PGC-1α or SIRT1 by using small inhibitory RNA and observed an attenuation of decreased oxygen consumption in CR serum-treated cells (Fig. 5, which is published as supporting information on the PNAS web site).

These *in vitro* results provide strong evidence to support how CR might exert its antiaging effects *in vivo* (29). We propose then that CR activates diverse regulatory pathways that greatly enhance stress resistance via the SIRT1 pathway (19) and markedly improve bioenergetics through the activation of the PGC-1α pathway.

Methods

Cell Cultures. HeLa cells (American Type Culture Collection) and FaO cells (European Collection of Cell Cultures, Salisbury, U.K.) were cultured in high-glucose DMEM and RPMI medium 1640 (GIBCO/BRL) supplemented with 10% heat-inactivated FCS and antibiotic/antimycotic solution. Primary hepatocytes were prepared from three different cohorts of six 12-month-old Fischer 344 male rats (41), fed AL or 40% CR since weaning, seeded on collagen-coated dishes, and cultured in F12/DMEM. Rat serum was obtained and used as described (18).

ROS and $\Delta\Psi$m Determination. Flow cytometry determination of ROS and $\Delta\Psi$m was performed by using an Epics XL cytometer (Coulter). Intracellular ROS were determined by using Het, cH_2DCFDA, and dihydrorhodamine 123 (dH-rhod123) (Molecular Probes). HeLa cells were cultured with 10% AL or CR serum in DMEM for 48 h, incubated with 1 μM Het, 10 μg/ml cH_2DCFDA, or 10 μg/ml dH-rhod123 for the last 30 min of treatment, washed twice with cold HBSS, and detached with a cold HBSS-based nonenzymatic solution (Sigma). They were kept cool and quickly analyzed by flow cytometry. Oxidized Het (ethidium) was determined as FL3 (620 $\pm$ 30 nm), and both cH_2DCFDA and dH-rhod123 were detected as FL1 (525 $\pm$ 20 nm).

$\Delta\Psi$m was determined by using the specific dye JC1 (Molecular Probes). Cells were cultured as indicated above for 48 h and stained with 5 μg/ml JC1 for the last 15 min of treatment, washed, and detached as indicated above. $\Delta\Psi$m was determined by the ratiometric analysis of orange fluorescence emitted by JC1 aggregates (FL2, 585 $\pm$ 20 nm) and that emitted by the free probe (FL1, 525 $\pm$ 20 nm). At these conditions, disruption of $\Delta\Psi$m by incubation with the uncoupler carbonylcyanide *m*-chlorophenylhydrazone (100 μM) produced a shift from orange to red fluorescence and the decrease of the ratio FL2/FL1 (data not shown). For confocal visualization of JC1-stained cells, a Leica TCS LR confocal microscope was used.

Determination of Mitochondrial Mass. Mitochondrial mass was determined by using either fluorescent dye MTG or NAO staining as indicated (42, 43). For flow cytometry determination, cells were incubated with AL or CR serum as indicated above, detached, and fixed with 3.7% formaldehyde in HBSS for 15 min, washed three times by centrifugation at 500 $\times$ *g* for 5 min, and resuspended in HBSS, pH 7.4. Fixed cell suspensions were incubated with 20–40 nM MTG for 20–30 min at room temperature in the dark, washed twice as indicated above, and analyzed by flow cytometry. Staining after fixation permits the determination of dye incorporation caused only by mitochondrial mass independent of the $\Delta\psi$m. As control, the effect of the uncoupler carbonylcyanide *m*-chlorophenylhydrazone (10 μM) was determined to demonstrate $\Delta\Psi$m-independent staining of mitochondria.

Biochemical determination of mitochondrial mass was performed by measuring the citrate synthase activity in whole extracts from cells. The activity was measured spectrophotometrically at 412 nm at 30°C. Cell and liver homogenates were added to buffer containing 0.1 mM 5,5-dithio-bis-(2-nitrobenzoic) acid, 0.5 mM oxaloacetate, 50 μM EDTA, 0.31 mM acetyl CoA, 5 mM triethanolamine hydrochloride, and 0.1 M Tris·HCl, pH 8.1. Citrate synthase was expressed as nmol/min per mg of protein.

Immunocytochemistry. Immunostaining of cells with mitochondrial marker proteins, cytochrome *c* and cytochrome *c* oxidase, was also performed following previously reported staining procedures with minor modifications (44). After incubation, adherent cells to coverslips were fixed with 3.7% formaldehyde in PBS for 10 min. After four washes with PBS, cells were permeabilized with 0.1% saponin in PBS for 5 min at room temperature. Samples were washed again with PBS plus 0.05% Tween 20 and blocked with 5% goat serum in PBS for 30 min. Primary antibody anti-cytochrome *c* (Pharmingen) or anti-cytochrome *c* oxidase I (RDI, Flanders, NJ) were used at 1:100 to stain cells at 37°C for 1 h. After four washes with PBS-Tween 20, FITC-labeled secondary antibody was added (1:200), and samples were incubated for 1 h at 37°C. After three more washes with PBS, coverslips were mounted with Mowiol, and cells were visualized by confocal microscopy as described above.

Western Blotting. Whole cells were electrophoresed in a 10–15% acrylamide SDS/PAGE. Proteins were transferred to Immobilon membranes (Amersham Pharmacia). Rabbit anti-human catalase, sheep anti-human Cu/Zn SOD (Calbiochem), and mouse anti-β-tubulin (Boehringer-Mannheim Biochemica) antibodies were used to detect proteins by Western blotting. Proteins were electrophoresed, transferred to nitrocellulose membranes, and, after blocking O/N at 4°C, incubated with the respective antibody solution at 1:1,000 to 1:5,000 dilution. Then, membranes were probed with their respective antibody labeled with horseradish peroxidase (1:5,000 to 1:10,000). Immunolabeled proteins were detected by using a chemioluminiscence method (Bio-Rad). Protein concentration was determined by the Bradford method.

ATP Determination. The whole amount of ATP in cells was performed by using the ATP determination kit from Molecular Probes (see *Supporting Text*, which is published as supporting information on the PNAS web site). Cells were seeded as indicated and incubated for 48 h with sera. After harvesting by centrifugation at 4,500 $\times$ *g* for 5 min at 4°C, ATP was extracted by incubating cell pellets with 1% trichloroacetic acid (TCA)/4 mM EDTA solution for 10 min on ice. Cell extracts were centrifuged at 12,000 $\times$ *g* for 10 min at 4°C and used for ATP determination as indicated by the manufacturer. Interference of TCA on ATP determination was avoided by dilution of sample at least 1:10. The amount of ATP was determined by comparison with a curve obtained by using known amounts of ATP dissolved in the same buffer composition used for ATP extraction.

Oxygen Consumption Determination. Oxygen consumption of intact cells and hepatocytes was measured by using a Clark-type oxygen electrode containing a magnetic stirrer (Hansatech Instruments, Norfolk, U.K.) or monitored with an Instech Two Channel Fiber Optic Oxygen Monitor System (Instech Laboratories, Plymouth Meeting, PA). Cell chambers were maintained at 37°C by a circulating water bath. All measurements were assessed with fiber

optic oxygen monitor operating software and slope calculator software (Instech Laboratories). Respiration rates were completed in 0.25-ml suspensions of cells, and results were calculated as nmol of oxygen consumed per min per 10^6 cells. Resting respiration rate was determined as the oxygen consumption rate under conditions where no inhibitors or uncouplers were added to the cells. Nonmitochondrial oxygen consumption was determined as the respiration rate after incubation of cells with oligomycin (1 μg/ml), antimycin (5 μM), valinomycin (0.1 μM), and carbonyl *p*-trifluoromethoxyphenylhydrazone (20 μM). Mitochondrial respiration was calculated by subtracting nonmitochondrial respiration rates from measures of total respiration.

Determination of mRNA for Mitochondrial Biogenesis Factors. Total RNA from cells cultures with AL or CR serum and liver were extracted by using Tripure Reagent (Roche Diagnostics). Reverse transcriptase (RT) was performed by using 3 μg of total RNA for RT with oligo-18(dT) as primer. PCR was performed with specific primers for human NRF1 (forward, 5′-CCAAACCGAACATATGGCTCAC-3′; reverse, 5′-CCAGGATCATGCTCTTGTAC-3′); human NRF2α (forward, 5′-TAGACCTCACCACACTCAAC-3′; reverse, 5′-GTGACCAAACGGTTCAACTC-3′); human NRF2$\beta\gamma$ (forward, GAGCTCCCTTTACTACAGAC-3′; reverse, 5′-AACTGTGGTGTTGCAGCAT-3′); human PPARα (forward, 5′-GCTTTGGCTTTACGGAATA-3′; reverse, 5′-TCCCGACAGAAAGGCACT-3′); and human GAPDH (forward, 5′-CGGAGTCAACGGATTTGGTC-3′; reverse, 5′-ACTGTGGTCATGAGTGGTTC-3′) synthesized by Proligo (Boulder, CO) as described (34). PCR was carried out in a thermocycler in a 25-μl reaction volume containing 1 μl of cDNA, BioTaq PCR buffer, 50 μM of each dNTP, 1.25 mM $MgCl_2$, and 1 unit of BioTaq DNA polymerase (BioLine, Randolph, MA). The samples were also tested without RT to verify that there was no contamination with genomic DNA. The thermal cycle profile consisted of an initial denaturation step (1 min at 94°C), followed by 30 cycles (1 min of denaturation at 94°C, 1 min of annealing at 55°C, and 1 min of extension at 72°C) and a final extension step of 7 min at 72°C. The number of cycles was previously determined empirically to obtain a PCR product in the linear range. PCR products were resolved in an 1% agarose gel, scanned by using a Gel Doc 2000 device (Bio-Rad), and quantified by using QUANTITY ONE 1-D analysis software (Bio-Rad).

EM and Image Analysis. A cohort of six CR and eight AL 24-month-old male Fischer 344 rats were anaesthetized with pentobarbitone acepromazine malate. Livers were perfused with heparinized Krebs-Henseleit solution under a constant pressure of 10 cm of water. One lobe was removed, fixed in 4% phosphate-buffered paraformaldehyde for 6 h, and then stored in PBS. The rest of the liver was fixed with a fixative solution for EM consisting of 3% glutaraldehyde, 2% paraformaldehyde, 2% sucrose, 2 M calcium chloride, and 0.1 M cacodylate buffer. After being fixed, part of the liver was removed, cut into 1-mm^3 sections, and postfixed for 6 h in the fixative solution. The samples were then stored in 0.1 M cacodylate buffer.

The formalin-fixed liver was later embedded in paraffin, sectioned, and stained with hematoxylin and eosin. Livers with abnormal pathology, such as a lymphocytic infiltrate, were excluded. The liver fixed for EM was postfixed in osmium tetraoxide (1%), dehydrated in an alcohol series, and embedded in Spurr's resin. Two blocks of the liver were selected randomly from those satisfying requirements for tissue integrity and quality of fixation (45). Ultrathin (70–90 nm) sections were then taken from each block, stained with uranyl acetate and lead citrate, and then blinded for the observer and viewed on a Zeiss 902 electron microscope. Two random hepatocytes from each section were captured, at ×4,400 magnification, on a Gatan (Pleasanton, CA) BioScan slow scan charge-coupled device camera.

Statistical Analysis. Statistical analyses were performed by using a commercially available software package (STATVIEW, SAS Institute, Cary, NC). Two-tailed Student's tests were used for all analyses. Statistical significance was established as $P < 0.05$.

This work was supported by the Intramural Research Program of the National Institute on Aging, the National Institutes of Health, and Spanish Ministerio de Ciencia y Tecnología Grant BMC2002-01602.

1. Nicholls, D. G. (2004) *Aging Cell* **3,** 35–40.
2. Salvioli, S., Bonafe, M., Capri, M., Monti, D. & Franceschi, C. (2001) *FEBS Lett* **492,** 9–13.
3. Lenaz, G., D'Aurelio, M., Merlo Pich, M., Genova, M. L., Ventura, B., Bovina, C., Formiggini, G. & Parenti Castelli, G. (2000) *Biochim. Biophys. Acta* **1459,** 397–404.
4. Sohal, R. S., Svensson, I. & Brunk, U. T. (1990) *Mech. Ageing Dev.* **53,** 209–215.
5. Weindruch, R. & Sohal, R. S. (1997) *N. Engl. J. Med.* **337,** 986–994.
6. Sohal, R. S. & Weindruch, R. (1996) *Science* **273,** 59–63.
7. Masoro, E. J. (2000) *Exp. Gerontol.* **35,** 299–305.
8. Lopez-Torres, M., Gredilla, R., Sanz, A. & Barja, G. (2002) *Free Radical Biol. Med.* **32,** 882–889.
9. Ramsey, J. J., Harper, M. E. & Weindruch, R. (2000) *Free Radical Biol. Med.* **29,** 946–968.
10. Schriner, S. E., Linford, N. J., Martin, G. M., Treuting, P., Ogburn, C. E., Emond, M., Coskun, P. E., Ladiges, W., Wolf, N., Van Remmen, H., *et al.* (2005) *Science* **308,** 1909–1911.
11. Orr, W. C., Mockett, R. J., Benes, J. J. & Sohal, R. S. (2003) *J. Biol. Chem.* **278,** 26418–26422.
12. Orr, W. C. & Sohal, R. S. (1994) *Science* **263,** 1128–1130.
13. Lin, S. J., Kaeberlein, M., Andalis, A. A., Sturtz, L. A., Defossez, P. A., Culotta, V. C., Fink, G. R. & Guarente, L. (2002) *Nature* **418,** 344–348.
14. Higami, Y., Pugh, T. D., Page, G. P., Allison, D. B., Prolla, T. A. & Weindruch, R. (2004) *FASEB J.* **18,** 415–417.
15. Hagopian, K., Harper, M. E., Ram, J. J., Humble, S. J., Weindruch, R. & Ramsey, J. J. (2005) *Am. J. Physiol.* **288,** E674–E684.
16. Lambert, A. J. & Merry, B. J. (2005) *J. Gerontol. A Biol. Sci. Med. Sci.* **60,** 175–180.
17. Lambert, A. J., Wang, B., Yardley, J., Edwards, J. & Merry, B. J. (2004) *Exp. Gerontol.* **39,** 289–295.
18. de Cabo, R., Furer-Galban, S., Anson, R. M., Gilman, C., Gorospe, M. & Lane, M. A. (2003) *Exp. Gerontol.* **38,** 631–639.
19. Cohen, H. Y., Miller, C., Bitterman, K. J., Wall, N. R., Hekking, B., Kessler, B., Howitz, K. T., Gorospe, M., De Cabo, R. & Sinclair, D. A. (2004) *Science* **305,** 390–392.
20. Lambert, A. J. & Merry, B. J. (2004) *Am. J. Physiol.* **286,** R71–R79.
21. Korshunov, S. S., Skulachev, V. P. & Starkov, A. A. (1997) *FEBS Lett.* **416,** 15–18.
22. Liu, S. S. (1997) *Biosci. Rep.* **17,** 259–272.
23. Bevilacqua, L., Ramsey, J. J., Hagopian, K., Weindruch, R. & Harper, M. E. (2005) *Am. J. Physiol.* **289,** E429–E438.
24. Bevilacqua, L., Ramsey, J. J., Hagopian, K., Weindruch, R. & Harper, M. E. (2004) *Am. J. Physiol.* **286,** E852–E861.
25. Weindruch, R., Walford, R. L., Fligiel, S. & Guthrie, D. (1986) *J. Nutr.* **116,** 641–654.
26. Duffy, P. H., Feuers, R. J., Leakey, J. A., Nakamura, K., Turturro, A. & Hart, R. W. (1989) *Mech. Ageing Dev.* **48,** 117–133.
27. Rumsey, W. L., Kendrick, Z. V. & Starnes, J. W. (1987) *Exp. Gerontol.* **22,** 271–287.
28. Lane, M. A., Baer, D. J., Rumpler, W. V., Weindruch, R., Ingram, D. K., Tilmont, E. M., Cutler, R. G. & Roth, G. S. (1996) *Proc. Natl. Acad. Sci. USA* **93,** 4159–4164.
29. Weindruch, R., Keenan, K. P., Carney, J. M., Fernandes, G., Feuers, R. J., Floyd, R. A., Halter, J. B., Ramsey, J. J., Richardson, A., Roth, G. S. & Spindler, S. R. (2001) *J. Gerontol. A. Biol. Sci. Med. Sci.* **56,** 20–33.
30. Nemoto, S., Fergusson, M. M. & Finkel, T. (2005) *J. Biol. Chem.* **280,** 16456–16460.
31. Rodgers, J. T., Lerin, C., Haas, W., Gygi, S. P., Spiegelman, B. M. & Puigserver, P. (2005) *Nature* **434,** 113–118.
32. Au, H. C. & Scheffler, I. E. (1998) *Eur. J. Biochem.* **251,** 164–174.
33. Scarpulla, R. C. (2002) *Biochim. Biophys. Acta* **1576,** 1–14.
34. Bergeron, R., Ren, J. M., Cadman, K. S., Moore, I. K., Perret, P., Pypaert, M., Young, L. H., Semenkovich, C. F. & Shulman, G. I. (2001) *Am. J. Physiol.* **281,** E1340–E1346.
35. Gulick, T., Cresci, S., Caira, T., Moore, D. D. & Kelly, D. P. (1994) *Proc. Natl. Acad. Sci. USA* **91,** 11012–11016.
36. Zhu, M., Miura, J., Lu, L. X., Bernier, M., DeCabo, R., Lane, M. A., Roth, G. S. & Ingram, D. K. (2004) *Exp. Gerontol.* **39,** 1049–1059.
37. Sung, B., Park, S., Yu, B. P. & Chung, H. Y. (2004) *J. Gerontol. A Biol. Sci.* **59,** 997–1006.
38. Herzig, R. P., Scacco, S. & Scarpulla, R. C. (2000) *J. Biol. Chem.* **275,** 13134–13141.
39. Koubova, J. & Guarente, L. (2003) *Genes Dev.* **17,** 313–321.
40. Lambert, A. J., Wang, B. & Merry, B. J. (2004) *Biochem. Biophys. Res. Commun.* **316,** 1196–1201.
41. Berry, M. N. & Friend, D. S. (1969) *J. Cell Biol.* **43,** 506–520.
42. Spodnik, J. H., Wozniak, M., Budzko, D., Teranishi, M.-A., Karbowski, M., Nishizawa, Y., Usukura, J. & Wakabayashi, T. (2002) *Mitochondrion* **2,** 163–179.
43. Mancini, M., Anderson, B. O., Caldwell, E., Sedghinasab, M., Paty, P. B. & Hockenbery, D. M. (1997) *J. Cell Biol.* **138,** 449–469.
44. Sanchez-Alcazar, J. A., Schneider, E., Hernandez-Munoz, I., Ruiz-Cabello, J., Siles-Rivas, E., de la Torre, P., Bornstein, B., Brea, G., Arenas, J., Garesse, R., *et al.* (2003) *Biochem. J.* **370,** 609–619.
45. Cogger, V. C., Warren, A., Fraser, R., Ngu, M., McLean, A. J. & Le Couteur, D. G. (2003) *Exp. Gerontol.* **38,** 1101–1107.